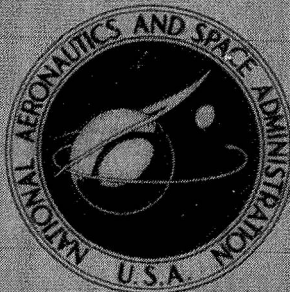




DECLASSIFIED



NASA TECHNICAL  
MEMORANDUM



NASA TM X-1080

NASA TM X-1080

N70-78336

FACILITY FORM 602	(ACCESSION NUMBER)	(THRU)
	20	NINE
	(PAGES)	(CODE)
	(NASA CR OR TMX OR AD NUMBER)	(CATEGORY)

Declassified by authority of NASA  
Classification Change Notices No. 310  
Dated \*\*12-15-70

LONGITUDINAL AERODYNAMIC  
CHARACTERISTICS OF A  
MANNED LIFTING ENTRY VEHICLE  
AT A MACH NUMBER OF 19.7

by *Julius E. Harris*  
*Langley Research Center*  
*Langley Station, Hampton, Va.*

UNCLASSIFIED  
10/23/70  
10/23/70



LONGITUDINAL AERODYNAMIC CHARACTERISTICS  
OF A MANNED LIFTING ENTRY VEHICLE  
AT A MACH NUMBER OF 19.7 (6)

By Julius E. Harris

Langley Research Center  
Langley Station, Hampton, Va.



NATIONAL AERONAUTICS AND SPACE ADMINISTRATION



LONGITUDINAL AERODYNAMIC CHARACTERISTICS  
OF A MANNED LIFTING ENTRY VEHICLE

AT A MACH NUMBER OF 19.7\*

By Julius E. Harris  
Langley Research Center

SUMMARY

14146

An experimental investigation has been conducted to determine the static longitudinal aerodynamic characteristics of a manned lifting entry configuration designated HL-10 (horizontal lander 10). The tests were made in the Langley hotshot tunnel at a Mach number of approximately 19.7 and a Reynolds number, based on model length, of  $0.2 \times 10^6$  for angles of attack from  $10^\circ$  to  $45^\circ$  and elevon deflections of  $-60^\circ$ ,  $0^\circ$ , and  $30^\circ$ .

Trimmed lift-drag ratios for the present investigation for elevon deflections of  $30^\circ$  and  $0^\circ$  were 0.96 and 0.78; trimmed lift coefficients corresponding to these lift-drag ratios were 0.27 and 0.48, respectively. The trim point for an elevon deflection of  $-60^\circ$  was not reached in the angle-of-attack range of the investigation. Comparison of some of the data from the present investigation with data from previous investigations indicated a substantial loss in elevon effectiveness for a deflection of  $30^\circ$  for the present investigation; this loss in effectiveness is attributed to laminar flow separation. An unexplained divergence existed between the results of the present investigation and those of previous investigations for angles of attack greater than  $30^\circ$  and elevon deflections of  $0^\circ$  and  $-60^\circ$ . Conf

*Adt*

INTRODUCTION

Recent studies have indicated that an entry vehicle with hypersonic lift-drag ratio of about 1 may have application for future space missions. Consequently, a general research study of a vehicle of this class was undertaken at the Langley Research Center to ascertain problem areas, to seek their solutions, and to develop a promising configuration. To provide a focal point for these objectives, a configuration has been evolved through work of the type reported in references 1 to 3. This configuration was designated the basic HL-10.


The purpose of the present investigation was to study the longitudinal aerodynamic characteristics of the basic HL-10 configuration at a Mach number of approximately 19.7 and a Reynolds number, based on body length, of approximately  $0.2 \times 10^6$ .

# SYMBOLS

The axial-force, normal-force, and pitching-moment data are referred to the body system of axes, whereas the lift and drag data are referred to the stability system of axes. In deriving the coefficients, the reference area used was the planform area (including elevons) of 22.84 square inches and the reference length used was the model length of 8 inches.

$C_A$	axial-force coefficient, $\frac{F_A}{q_\infty S}$
$C_D$	drag coefficient, $\frac{F_D}{q_\infty S}$
$C_L$	lift coefficient, $\frac{F_L}{q_\infty S}$
$C_m$	pitching-moment coefficient, $\frac{\text{Pitching moment}}{q_\infty S l}$
$C_N$	normal-force coefficient, $\frac{F_N}{q_\infty S}$
$F_A$	axial force
$F_D$	drag force, $F_N \sin \alpha + F_A \cos \alpha$
$F_L$	lift force, $F_N \cos \alpha - F_A \sin \alpha$
$F_N$	normal force
$l$	model reference length
$L/D$	lift-drag ratio
$M_\infty$	free-stream Mach number
$p_\infty$	free-stream static pressure
$p_{t,1}$	total pressure ahead of normal shock





$q_\infty$	free-stream dynamic pressure, $\frac{1}{2}\rho_\infty V_\infty^2$
$R_\infty$	Reynolds number, $\frac{\rho_\infty V_\infty l}{\mu_\infty}$
$S$	reference planform area, including area of elevons
$S_e$	elevon area
$T_\infty$	free-stream static temperature
$T_{t,1}$	total temperature ahead of normal shock
$V_\infty$	free-stream velocity
$X, Y, Z$	body axes (see fig. 4)
$x_{cp}$	center-of-pressure location, measured from nose
$\alpha$	angle of attack
$\gamma$	ratio of specific heats
$\mu_\infty$	free-stream static coefficient of viscosity
$\rho_\infty$	free-stream static density
$\delta_e$	elevon deflection angle, positive with trailing edge down

#### APPARATUS AND TESTS

The present investigation was conducted at the Langley Research Center in the Langley hotshot tunnel. This facility will be briefly discussed in the following paragraphs. The reader interested in a more detailed discussion is referred to reference 4.

The Langley hotshot tunnel is an arc-heated, hypervelocity blowdown tunnel. The major components include a capacitor bank for storage of electrical energy, an arc-heated reservoir, a  $10^\circ$  conical nozzle and test section, a 24-inch cylindrical test section, a diffuser, and a 300-cubic-foot vacuum chamber. A sketch of the facility is presented as figure 1. The operation of the facility for the present investigation was as follows: First, the tunnel and vacuum chamber were evacuated to approximately 5 microns of mercury, and the arc chamber pressurized with nitrogen gas to 1000 psia at  $530^\circ$  R. Next, the capacitor storage system was charged to the desired energy level and then discharged across the electrodes in the arc chamber. This arc discharge heated and pressurized the


nitrogen to approximately 5400° R and 11,000 psia, respectively. The high enthalpy nitrogen then ruptured a diaphragm separating the arc chamber from the nozzle and expanded through the conical nozzle to a Mach number of approximately 19.7 in the test section for a run time of approximately 0.1 second.

A three-component, internally mounted strain-gage balance was used to measure the forces and moments during the investigation. The strain-gage outputs were amplified by 3-kilocycle carrier amplifiers and recorded on an oscillograph. A photograph of the model and balance assembly is presented as figure 2. The total pressure in the arc chamber was measured with strain-gage pressure transducers during each test. This pressure, together with the initial arc-chamber density prior to arc discharge, was used to calculate the total temperature. The total pressure behind the normal shock in the test section was measured with variable-reluctance pressure transducers. This pressure, together with the arc-chamber conditions of total temperature and pressure, was used to calculate the free-stream Mach number. Base pressure was not measured during the investigation.

The approximate test conditions for the present investigation are listed in the following table:

$\alpha$	10° to 45°
$\delta_e$	-60°, 0°, and 30°
$\gamma$	1.40
$M_\infty$	19.7
$R_\infty$	$0.2 \times 10^6$
$p_{t,1}$	11,000 psia
$p_\infty$	0.002 psia
$T_{t,1}$	5400° R
$T_\infty$	87° R

The maximum anticipated uncertainties in the force and moment coefficients resulting from any error in the strain-gage-balance measurements, the carrier-amplifier outputs, and the pitot-pressure measurements are



$C_N$ . . . . .	$\pm 0.01$
$C_A$ . . . . .	$\pm 0.01$
$C_m$ . . . . .	$\pm 0.001$

The maximum error in the angle of attack was less than  $\pm 0.1^\circ$ .

The model used in the present investigation was a blunt-leading-edge  $74^\circ$  delta planform with a negative-cambered flat bottom. Photographs of the model are presented as figures 2 and 3. The model was constructed of fiber glass with magnesium and steel reinforcement and had a mass of 140 grams. The elevons were constructed of stainless steel. The tip dorsal fins, of the type designated fin D in reference 3, were toed-in  $16^\circ$  and rolled out  $60^\circ$  from the horizontal. Drawings of the model are presented in figure 4, and a table of body coordinates is presented in reference 2.

## RESULTS AND DISCUSSION

The basic results are presented in figures 5 and 6 where they are referred to the body axes and to the stability axes, respectively.

Trim angles of attack for elevon deflections of  $30^\circ$  and  $0^\circ$  were approximately  $30^\circ$  and  $47^\circ$ . (See fig. 5(a).) The  $47^\circ$  trim angle was obtained by extrapolating the curve for  $C_m$  to  $C_m = 0$ , since the maximum angle of attack for the investigation was  $45^\circ$ . The trim angle of attack for  $\delta_e = -60^\circ$  was not reached in the angle-of-attack range under consideration. Trimmed lift-drag ratios (see fig. 6) were 0.96 and 0.78 (extrapolated) for elevon deflections of  $30^\circ$  and  $0^\circ$ ; trimmed lift coefficients corresponding to these values were 0.27 and 0.48, respectively.

A comparison of the stability results obtained in the present investigation with those presented in reference 3 and with unpublished data from the Langley 22-inch helium tunnel is presented in figure 7. The trends established by the data for the  $30^\circ$  elevon deflections were in reasonably good agreement for the three facilities. However, the elevon effectiveness for  $\delta_e = 30^\circ$  was much less for the present results than for the two previous investigations. Although the schlieren photographs presented in figure 8 do not show sufficient flow-field details to evaluate the existence of laminar separation, it is believed that the loss in elevon effectiveness of the present investigation is a result of laminar flow separation at the test Reynolds number of  $0.2 \times 10^6$ . Flow direction is from right to left in the schlieren photographs, and the dark spots in the photographs are chips in the test-section windows.

The present data for  $\delta_e = 0^\circ$  are in agreement with the data from the two previous investigations for  $\alpha \leq 30^\circ$ . (See fig. 7.) For  $\alpha > 30^\circ$  and  $\delta_e = 0^\circ$  the data from reference 3 and the helium tunnel are in agreement, but the data from the present investigation indicate more positive values of  $C_m$ , which result in a trend of divergence from the reference data that increases with increasing angle of attack. The same trend may be noted for  $\delta_e = -60^\circ$ .

Several possibilities were considered as the cause of this divergence. The schlieren photographs in figure 8 show no evidence of tunnel blockage; pitot-pressure measurements likewise appear to be free of blockage indications. The effect of source flow from the conical nozzle (see refs. 5 and 6) has also been considered as a possible cause of the divergence, along with the possibility of sting-interference effects. The reduction in negative  $C_m$  can be attributed to either source flow or sting interference, but the increase in  $C_N$  is not readily attributable to either. Therefore, the reason for the divergence is not presently known.

#### CONCLUDING REMARKS

The results of an experimental investigation to determine the static longitudinal aerodynamic characteristics of a manned lifting entry configuration (designated HL-10) have been presented. The investigation was made in the Langley hotshot tunnel at a Mach number of approximately 19.7 and a Reynolds number, based on model length, of approximately  $0.2 \times 10^6$  for angles of attack from  $10^\circ$  to  $45^\circ$  and elevon deflections of  $-60^\circ$ ,  $0^\circ$ , and  $30^\circ$ .

A brief analysis of the data from the present investigation and a comparison of the data with those from previous investigations have indicated the following concluding remarks:

1. Trimmed lift-drag ratios for elevon deflections of  $30^\circ$  and  $0^\circ$  were 0.96 and 0.78; trimmed lift coefficients corresponding to these lift-drag ratios were 0.27 and 0.48, respectively. The trim point for the elevon deflection of  $-60^\circ$  was not reached in the angle-of-attack range of the investigation.
2. A substantial loss in elevon effectiveness for a deflection of  $30^\circ$  was found to occur in the comparison with results from previous tests; this loss in effectiveness is attributed to laminar flow separation.
3. An unexplained divergence existed between the results of the present investigation and those of previous investigations for angles of attack greater than  $30^\circ$  and elevon deflections of  $0^\circ$  and  $-60^\circ$ .

Langley Research Center,  
National Aeronautics and Space Administration,  
Langley Station, Hampton, Va., December 23, 1964.



REFERENCES

1. Rainey, Robert W.; and Ladson, Charles L.: Preliminary Aerodynamic Characteristics of a Manned Lifting Entry Vehicle at a Mach Number of 6.8. NASA TM X-844, 1963.
2. Ware, George M.: Aerodynamic Characteristics of Models of Two Thick  $74^\circ$  Delta Manned Lifting Entry Vehicles at Low-Subsonic Speeds. NASA TM X-914, 1964.
3. Ladson, Charles L.: Aerodynamic Characteristics of a Manned Lifting Entry Vehicle at a Mach Number of 6.8. NASA TM X-915, 1964.
4. Smith, Fred M.; Harrison, Edwin F.; and Lawing, Pierce L.: Description and Initial Calibration of the Langley Hotshot Tunnel With Some Real-Gas Charts for Nitrogen. NASA TN D-2023, 1963.
5. Arrington, James P.; Joiner, Roy C., Jr.; and Henderson, Arthur, Jr.: Longitudinal Characteristics of Several Configurations at Hypersonic Mach Numbers in Conical and Contoured Nozzles. NASA TN D-2489, 1964.
6. Arrington, James P.; and Maddalon, Dal V.: Aerodynamic Characteristics of Several Lifting and Nonlifting Configurations at Hypersonic Speeds in Air and Helium. NASA TM X-918, 1964.

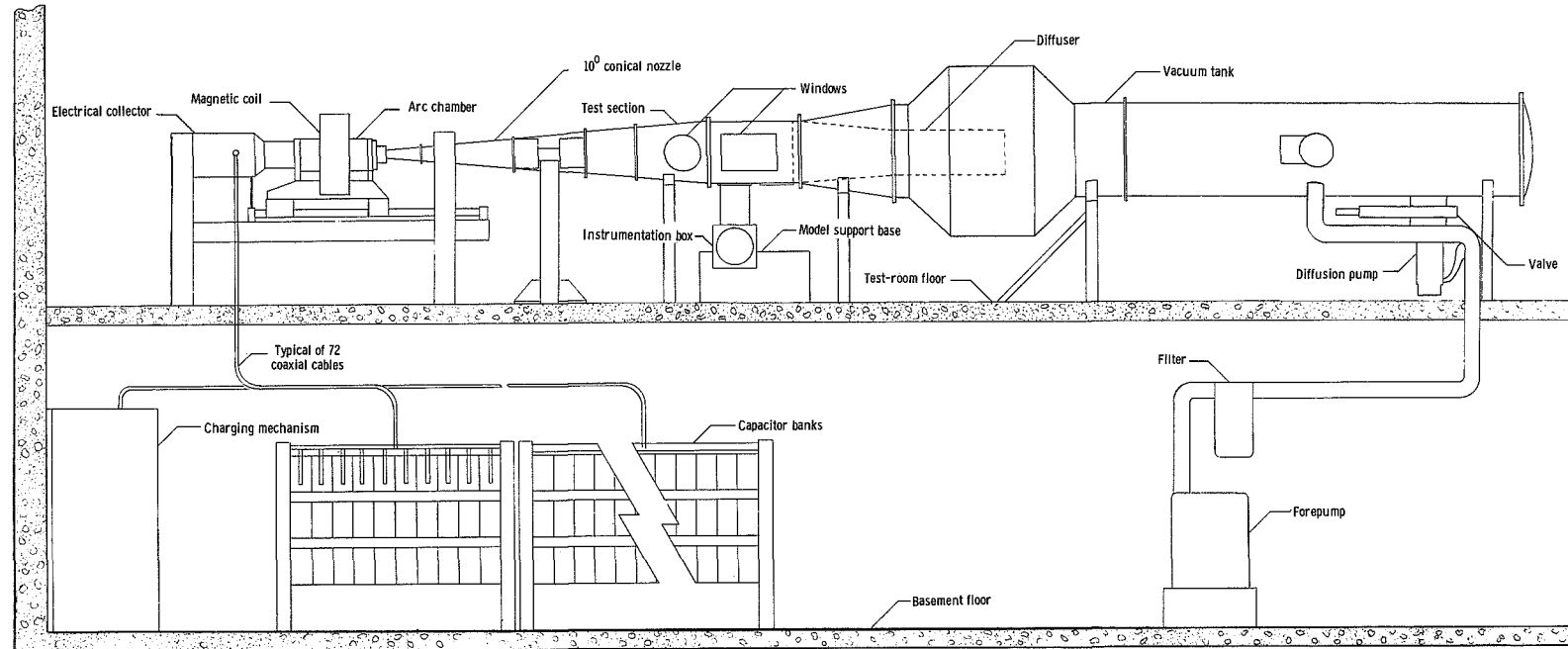


Figure 1.- Langley hotshot tunnel.

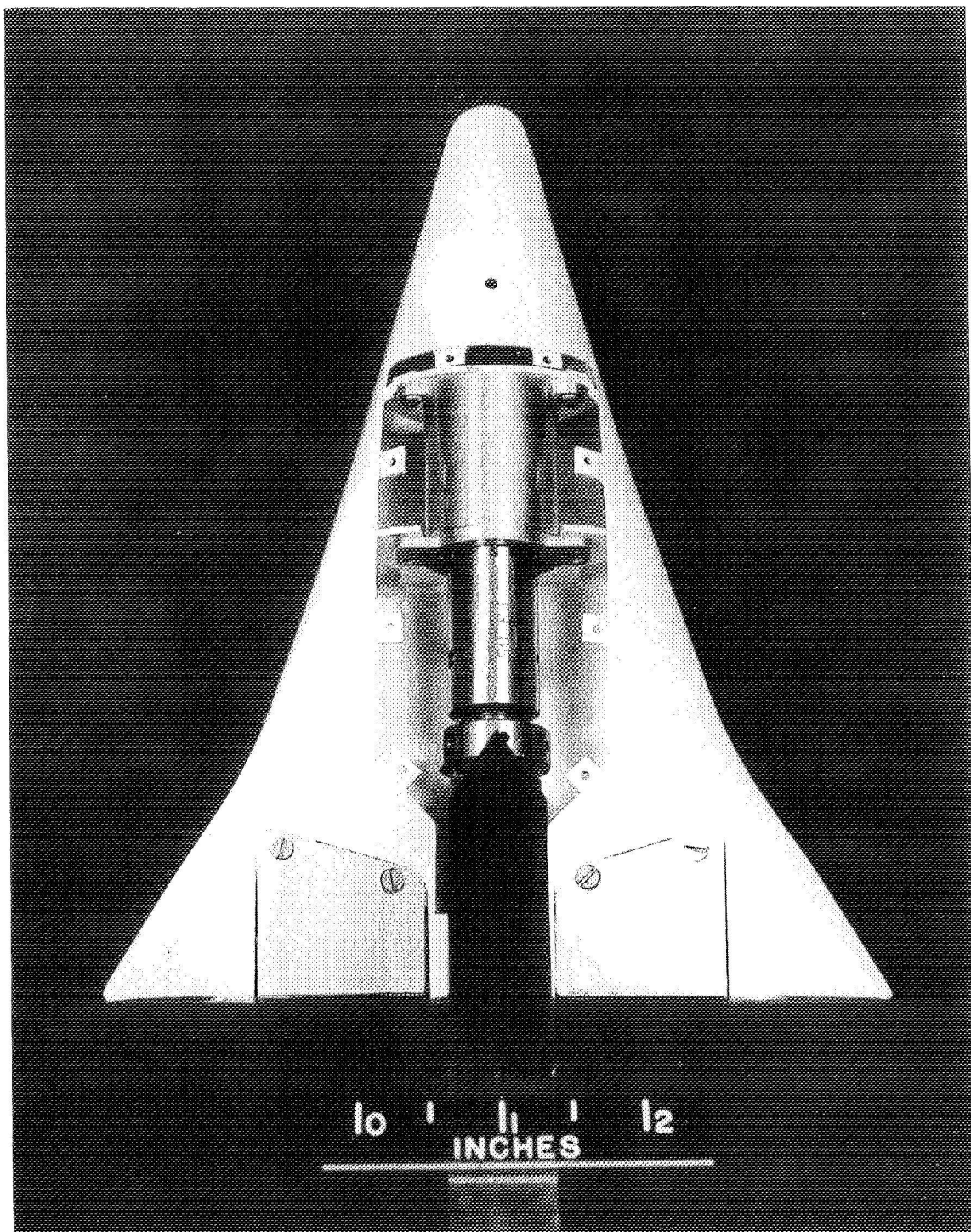


Figure 2.- Model and balance assembly.

L-64-3491

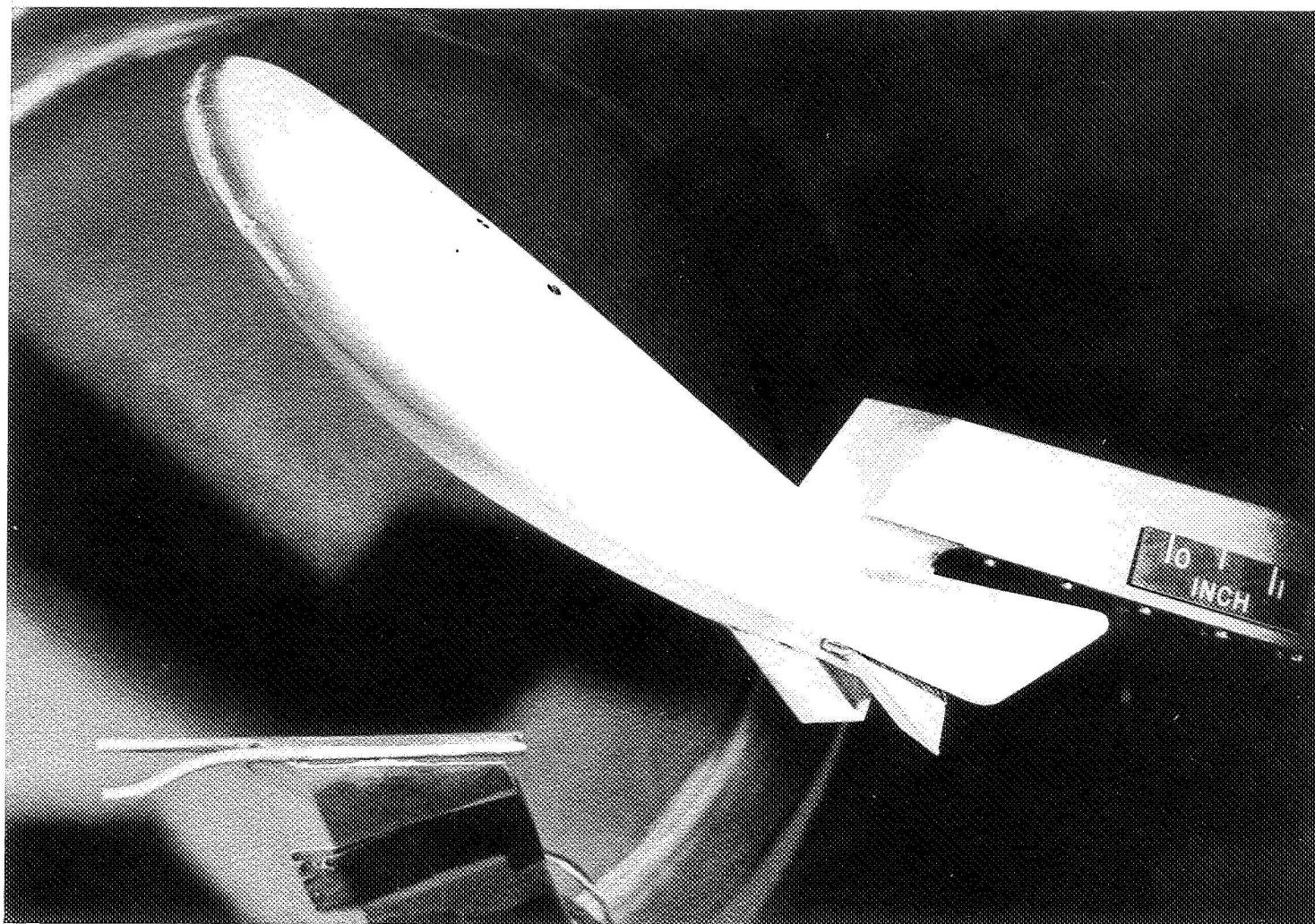
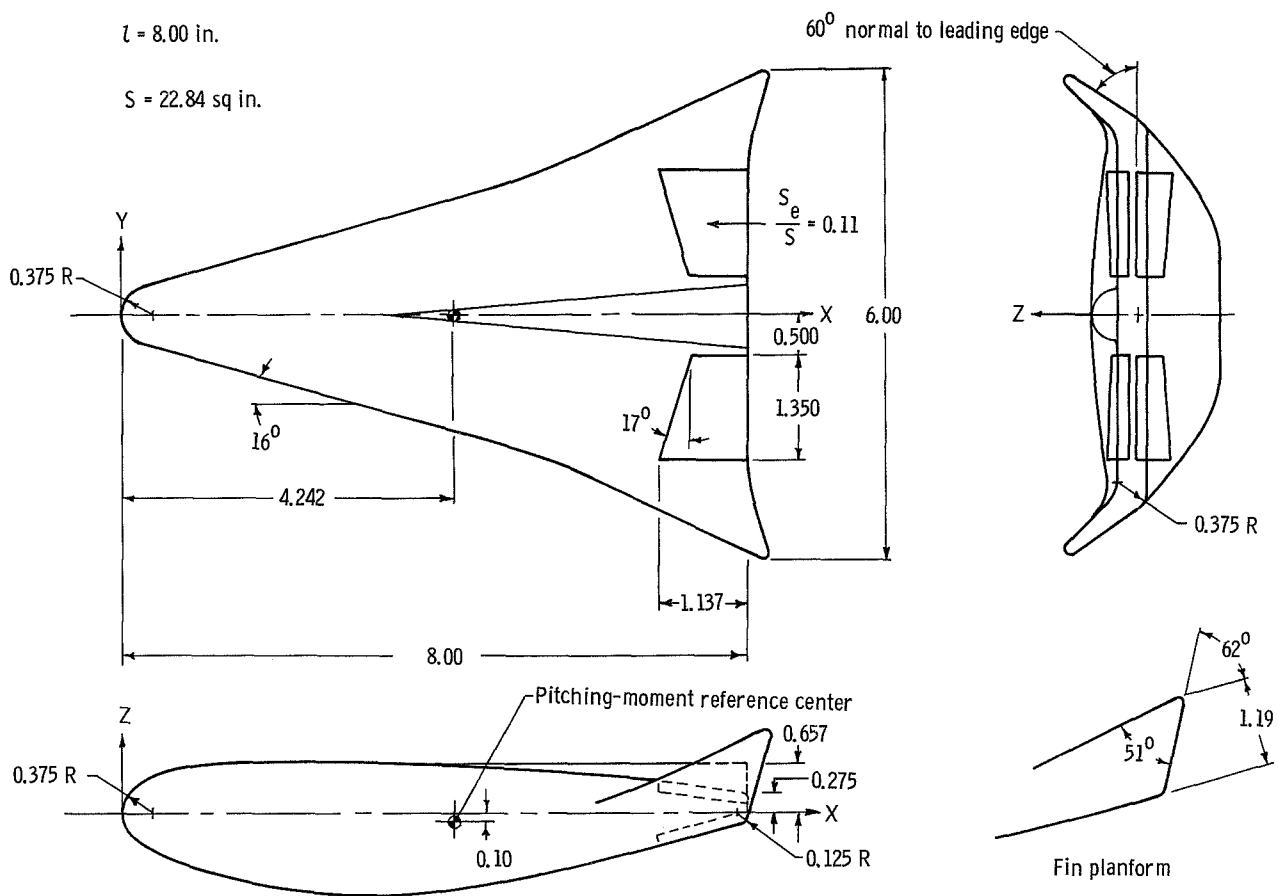


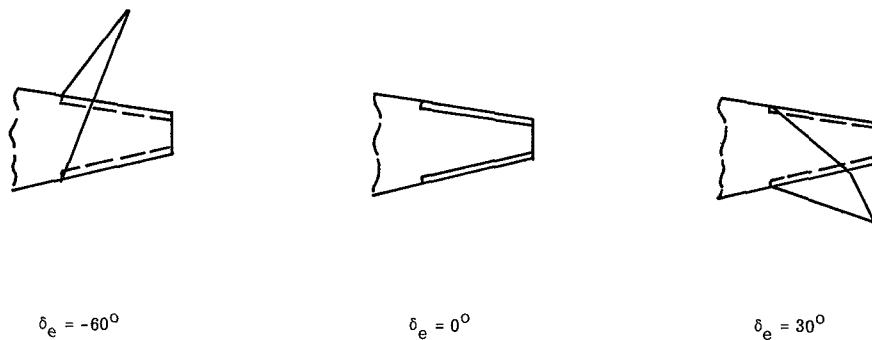
Figure 3.- Photograph of model in tunnel.

L-64-2481



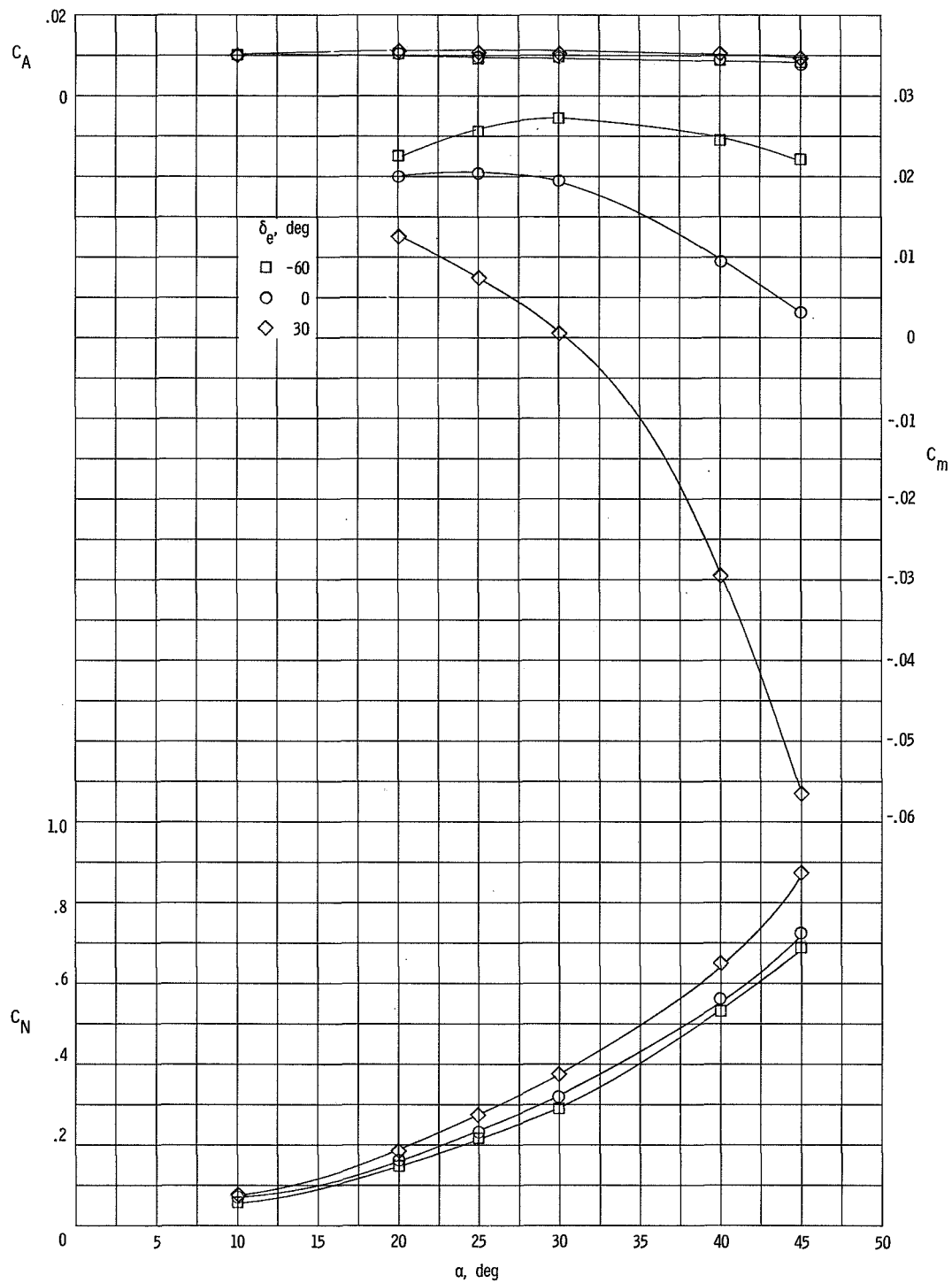


(a) Model dimensions.



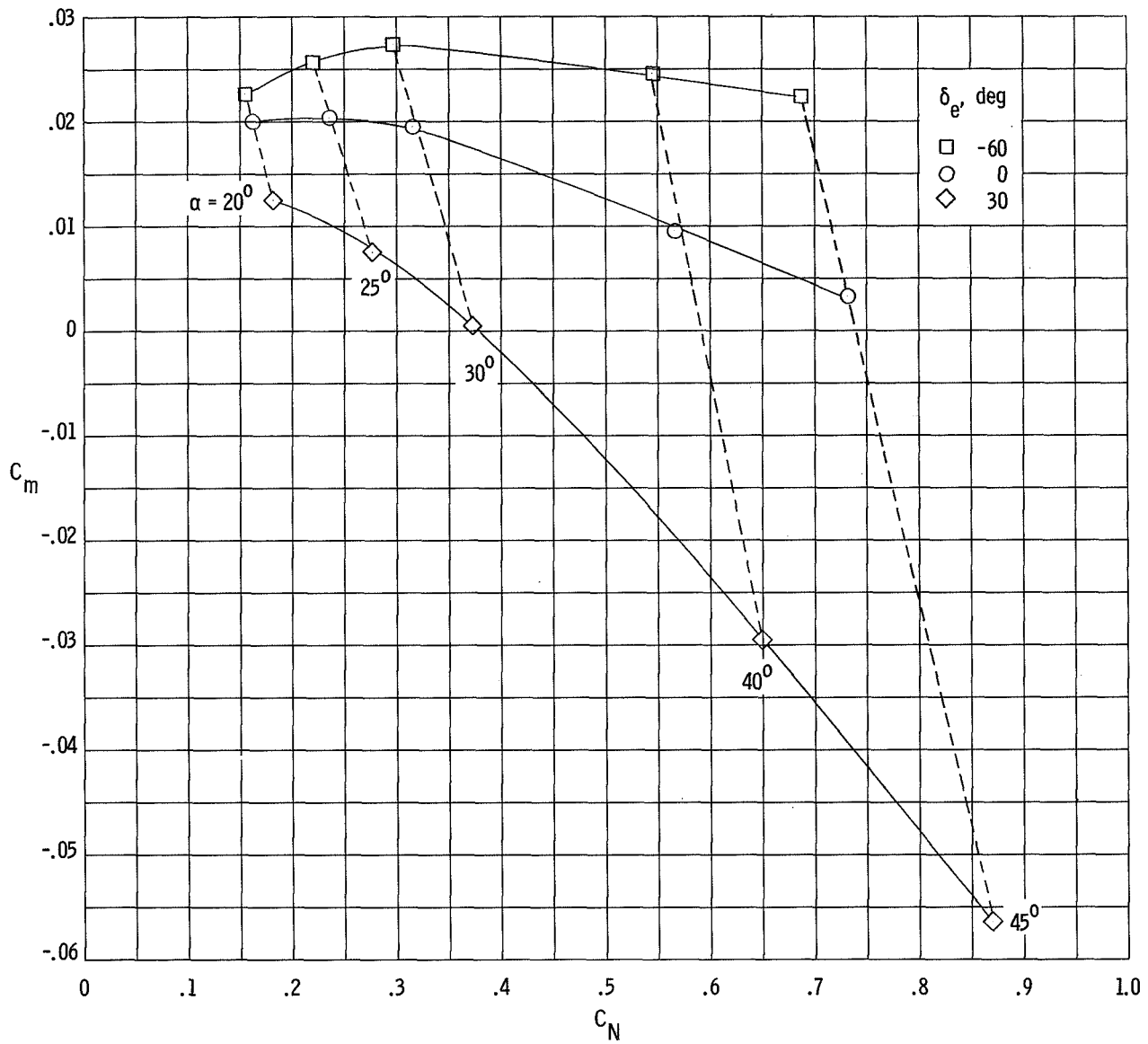
(b) Elevon deflections.

Figure 4.- Drawings of model. (All linear dimensions in inches.)



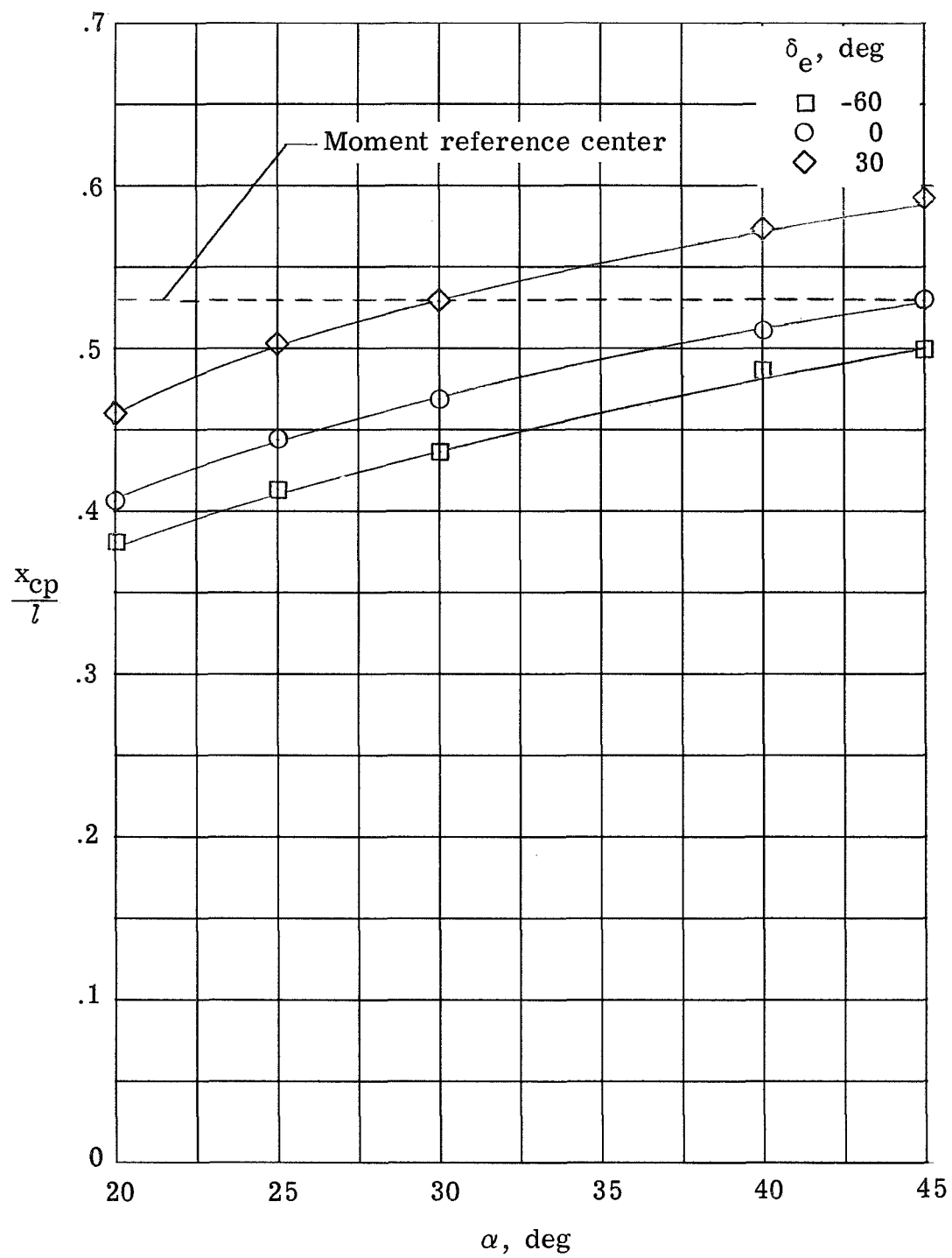
(a)  $C_N$ ,  $C_m$ , and  $C_A$ .

Figure 5.- Longitudinal aerodynamic characteristics referred to body axes.



(b) Stability characteristics.

Figure 5.- Continued.



(c) Center of pressure.

Figure 5.- Concluded.



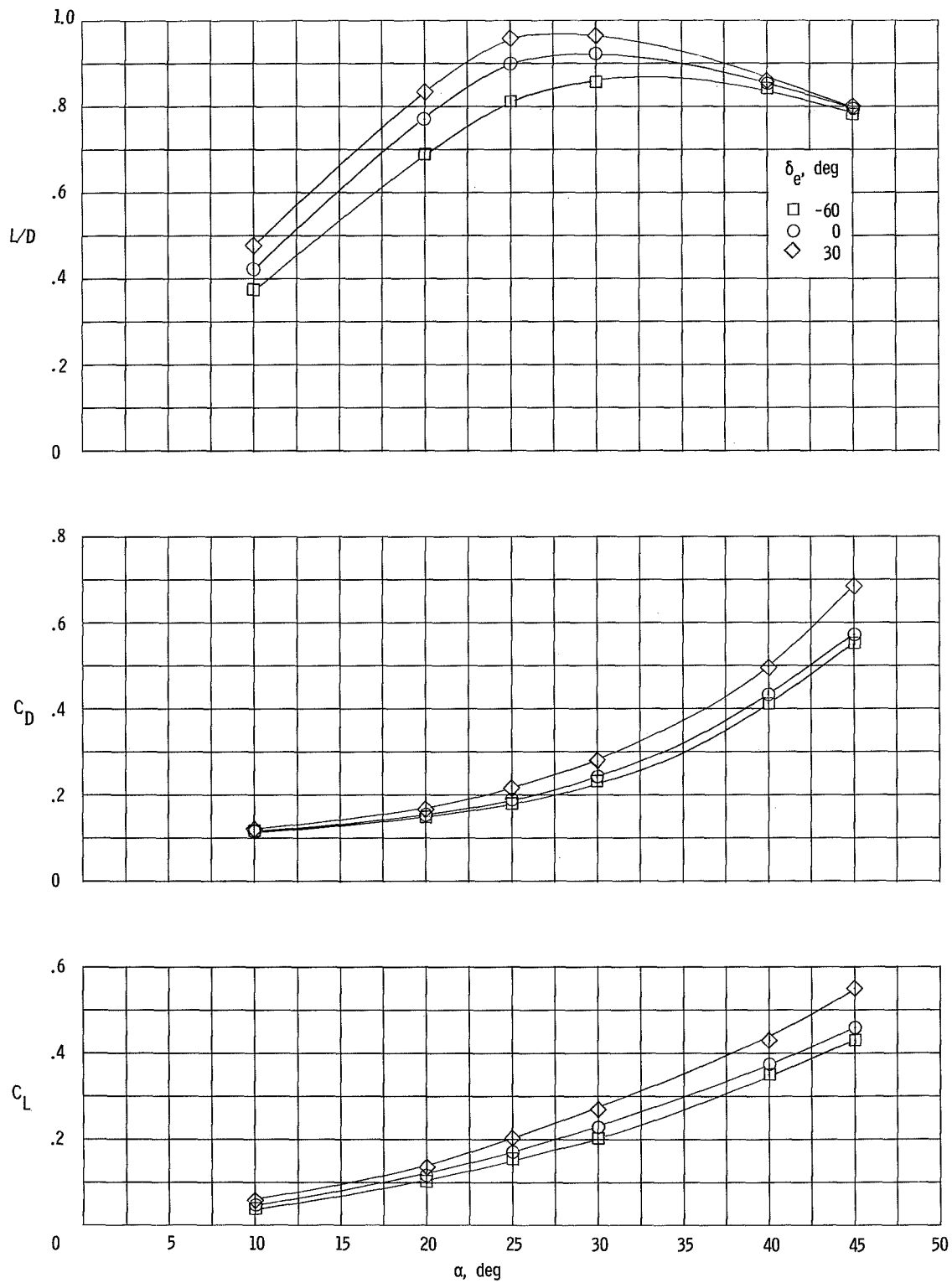


Figure 6.- Longitudinal aerodynamic characteristics referred to the stability axes.

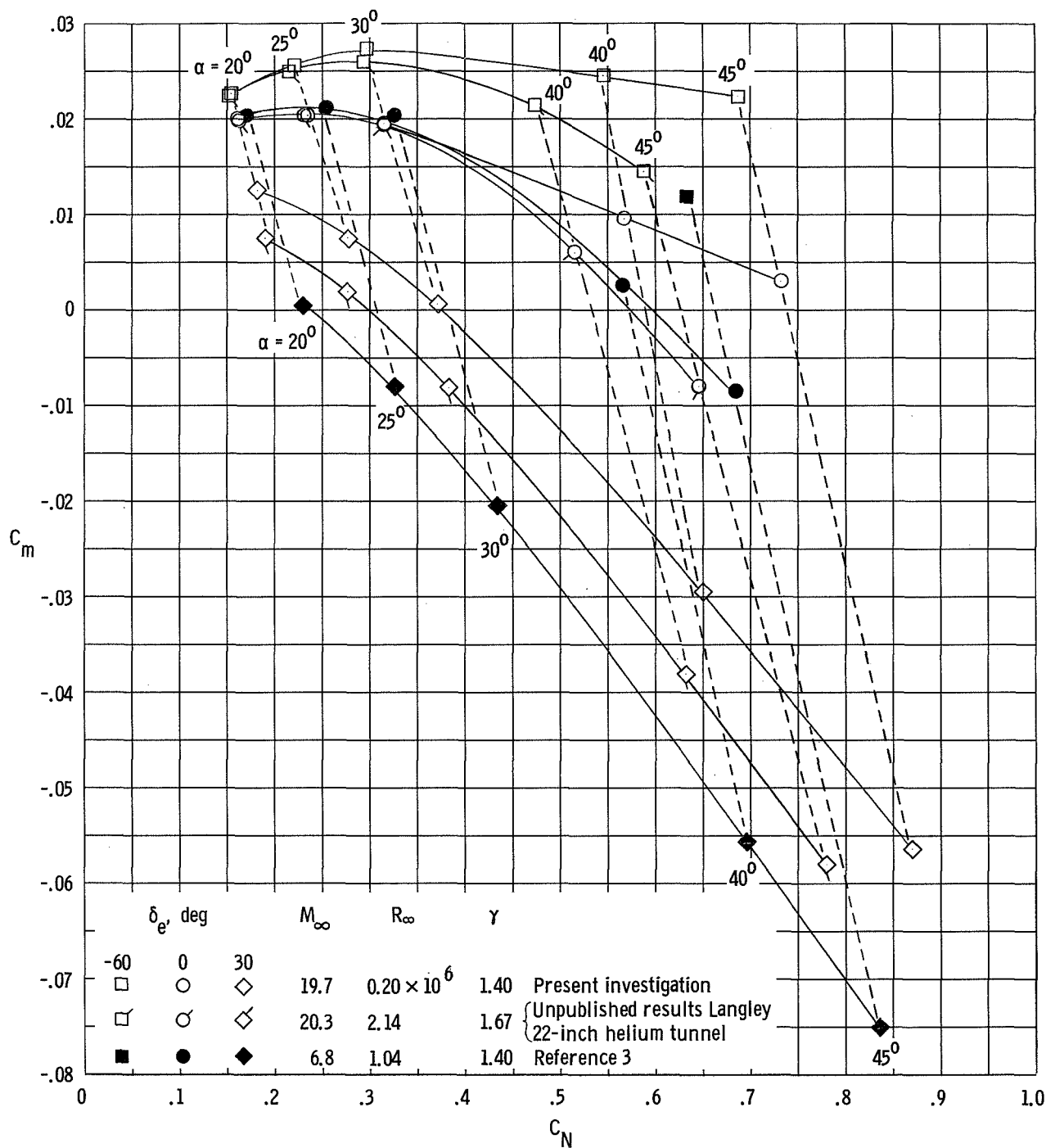
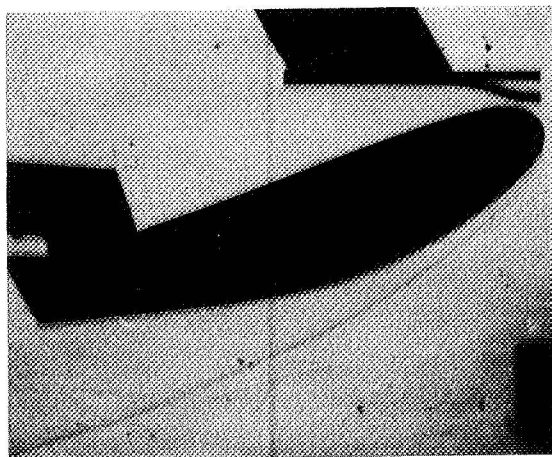
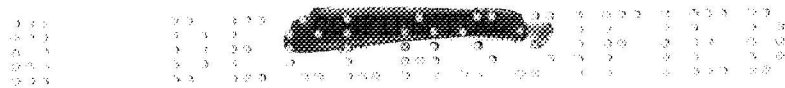
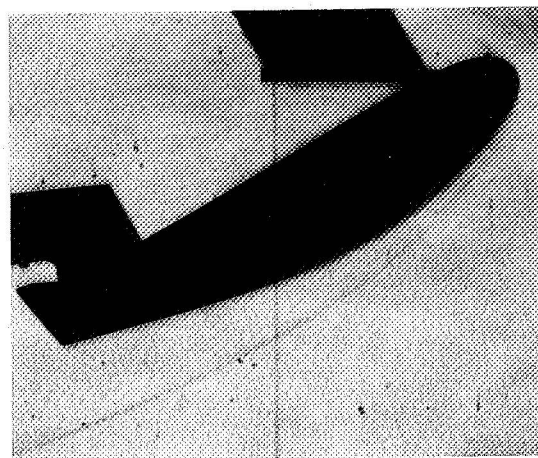


Figure 7.- Comparison of stability characteristics.

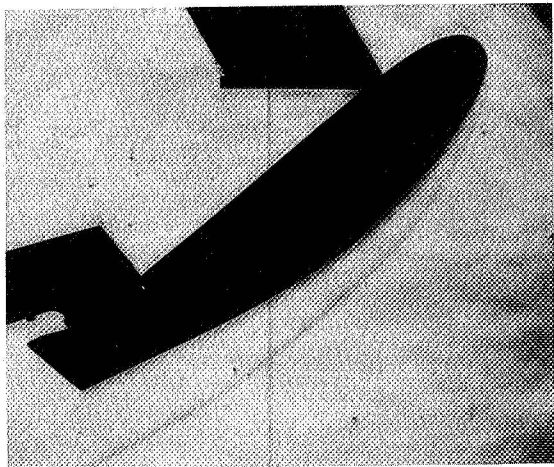


$\alpha = 20^\circ$

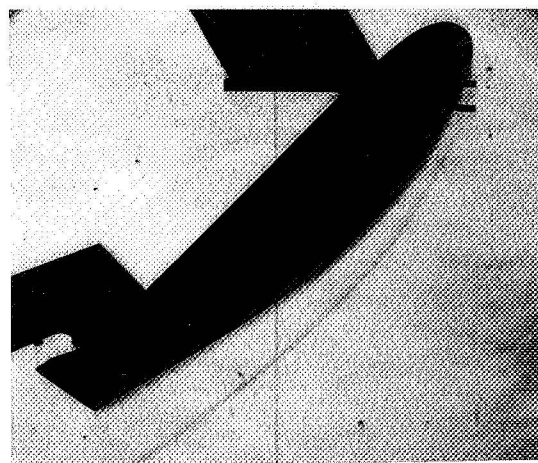


$\alpha = 30^\circ$

← Flow



$\alpha = 40^\circ$

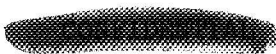


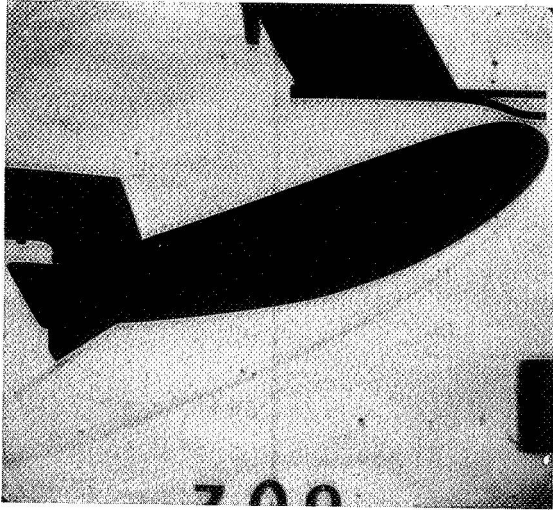
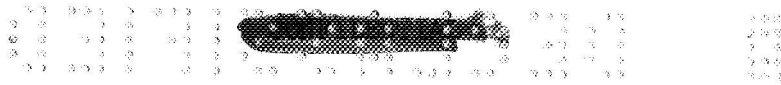
$\alpha = 45^\circ$

(a)  $\delta_e = 0^\circ$ .

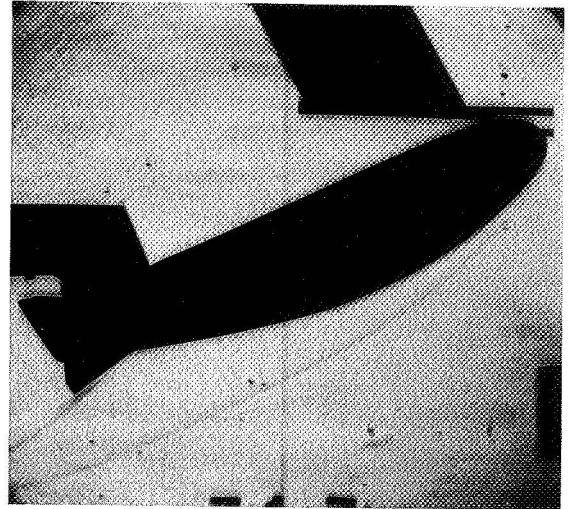
Figure 8.- Schlieren photographs.

L-65-8



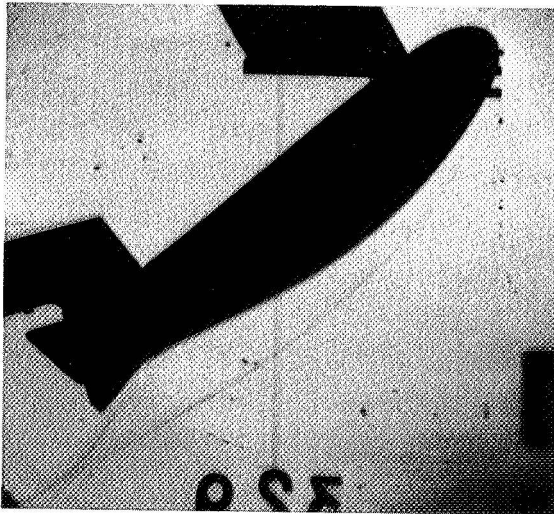


$\alpha = 20^{\circ}$



$\alpha = 25^{\circ}$

← Flow



$\alpha = 40^{\circ}$



$\alpha = 45^{\circ}$

(b)  $\delta_e = 30^{\circ}$ .

L-65-9

Figure 8.- Concluded.



*"The aeronautical and space activities of the United States shall be conducted so as to contribute . . . to the expansion of human knowledge of phenomena in the atmosphere and space. The Administration shall provide for the widest practicable and appropriate dissemination of information concerning its activities and the results thereof."*

—NATIONAL AERONAUTICS AND SPACE ACT OF 1958

## NASA SCIENTIFIC AND TECHNICAL PUBLICATIONS

**TECHNICAL REPORTS:** Scientific and technical information considered important, complete, and a lasting contribution to existing knowledge.

**TECHNICAL NOTES:** Information less broad in scope but nevertheless of importance as a contribution to existing knowledge.

**TECHNICAL MEMORANDUMS:** Information receiving limited distribution because of preliminary data, security classification, or other reasons.

**CONTRACTOR REPORTS:** Technical information generated in connection with a NASA contract or grant and released under NASA auspices.

**TECHNICAL TRANSLATIONS:** Information published in a foreign language considered to merit NASA distribution in English.

**TECHNICAL REPRINTS:** Information derived from NASA activities and initially published in the form of journal articles.

**SPECIAL PUBLICATIONS:** Information derived from or of value to NASA activities but not necessarily reporting the results of individual NASA-programmed scientific efforts. Publications include conference proceedings, monographs, data compilations, handbooks, sourcebooks, and special bibliographies.

*Details on the availability of these publications may be obtained from:*

SCIENTIFIC AND TECHNICAL INFORMATION DIVISION  
NATIONAL AERONAUTICS AND SPACE ADMINISTRATION

Washington, D.C. 20546